Biochemical and Biophysical Research Communications 453 (2014) 778–783

Contents lists available at ScienceDirect

Biochemical and Biophysical Research Communications

journal homepage: www.elsevier.com/locate/ybbrc

Lack of REDD1 reduces whole body glucose and insulin tolerance, and impairs skeletal muscle insulin signaling

Cory M. Dungan [a], David C. Wright [b], David L. Williamson [a,*]

[a] Department of Exercise and Nutrition Sciences, School of Public Health and Health Professions, University at Buffalo, Buffalo, NY, United States
[b] Department of Human Health and Nutrition Sciences, University of Guelph, Guelph, ON, Canada

ARTICLE INFO

Article history:
Received 25 September 2014
Available online 14 October 2014

Keywords:
mTOR
Akt
ERK1/2
RTP801
Insulin action

ABSTRACT

A lack of the REDD1 promotes dysregulated growth signaling, though little has been established with respect to the metabolic role of REDD1. Therefore, the goal of this study was to determine the role of REDD1 on glucose and insulin tolerance, as well as insulin stimulated growth signaling pathway activation in skeletal muscle. First, intraperitoneal (IP) injection of glucose or insulin were administered to REDD1 wildtype (WT) versus knockout (KO) mice to examine changes in blood glucose over time. Next, alterations in skeletal muscle insulin (IRS-1, Akt, ERK 1/2) and growth (4E-BP1, S6K1, REDD1) signaling intermediates were determined before and after IP insulin treatment (10 min). REDD1 KO mice were both glucose and insulin intolerant when compared to WT mice, evident by higher circulating blood glucose concentrations and a greater area under the curve following IP injections of glucose or insulin. While the REDD1 KO exhibited significant though blunted insulin-stimulated increases ($p < 0.05$) in Akt S473 and T308 phosphorylation versus the WT mice, acute insulin treatment has no effect ($p < 0.05$) on REDD1 KO skeletal muscle 4E-BP1 T37/46, S6K1 T389, IRS-1 Y1222, and ERK 1/2 T202/Y204 phosphorylation versus the WT mice. Collectively, these novel data suggest that REDD1 has a more distinct role in whole body and skeletal muscle metabolism and insulin action than previously thought.

1. Introduction

Skeletal muscle is a site for insulin action and glucose disposal and comprises a large portion of fat free mass. Skeletal muscle is positively associated with metabolic homeostasis [1], and the stability of muscle mass is central to insulin sensitivity and glucose metabolism [2]. Insulin regulates glucose uptake into skeletal muscle via the phosphatidylinositol-3 kinase (PI3K)/Akt pathway, resulting in the recruitment of glucose transporters to the plasma membrane [3]. Insulin also activates mammalian target of rapamycin (mTOR) through the PI3K–Akt pathway, which phosphorylates and inhibits the tuberous sclerosis complex 2 (TSC2), thus promoting GTPase activity of the mTOR kinase, Rheb [4]. mTOR is controlled by hormonal and nutrient cues, such as those altered during a fasted or a fed state [5], and regulates protein synthesis, autophagy, metabolism and cell survival [4]. mTOR exists in two interdependent multi-protein complexes, raptor containing mTOR complex 1 (mTORC1) and rictor containing mTOR complex 2 (mTORC2) [6,7]. mTORC1 phosphorylates two downstream substrates, the eukaryotic initiation factor (eIF) 4E binding protein-1 (4E-BP1) and p70 ribosomal protein S6 Kinase-1 (S6K1) [8]. Skeletal muscle from obese or insulin resistant rodents has an attenuated response to nutrient and growth stimuli [9–11], associated with dysregulated mTORC1 signaling. mTORC1 signaling activation should be reduced during a fasted state, though is hyperactive in obese and insulin resistant models [9–12]. Hyperactive mTORC1 negatively feeds back to inhibit the insulin receptor substrate-1 (IRS-1) by reducing tyrosine phosphorylation and promoting serine phosphorylation [9,12], downregulating insulin signaling.

A repressor of mTORC1, the protein regulated in development and DNA damage responses 1 (REDD1; also known as DDIT4 and RTP801) was initially reported as a stress-regulated protein [13] (e.g. hypoxia [14], glucocorticoids [15], DNA damage [16], endoplasmic reticulum (ER) stress [17]). However, recent findings have suggested a nutrient role for REDD1 [11,18,19] that is central to the insulin-mediated activation of Akt and mTOR. Our recent work [11] suggests that a loss of REDD1 limits skeletal muscle's ability to respond appropriately to nutrient cues. REDD1's exact mechanism of action on mTORC1 remains unclear, though recent findings [19] suggest that following a PP2A-dependent Akt T308 dephosphoryla-

* Corresponding author at: University at Buffalo, SUNY, School of Public Health and Health Professions, Department of Exercise and Nutrition Sciences, 2 Sherman Hall (office)/5 Sherman Hall (lab), Buffalo, NY 14214, United States. Fax: +1 716 829 2428.
E-mail address: davidwil@buffalo.edu (D.L. Williamson).

http://dx.doi.org/10.1016/j.bbrc.2014.10.032
0006-291X/

tion, reduced TSC2 phosphorylation promotes Rheb GTPase loading. Still, much remains to be determined about REDD1 and its role in metabolism. Thus, the goal of this study was to determine the role of REDD1 in the control of whole body glucose tolerance and skeletal muscle insulin action. We hypothesized that a loss of REDD1 leads to reductions in whole body glucose and insulin tolerance, and impairments in skeletal muscle insulin signaling.

2. Methods

2.1. Animals

The Institutional Animal Care and Use Committee at the University at Buffalo approved the protocols and procedures. All mice were housed at 21 °C in 50% humidity with 12/12 h light/dark cycle on a standard chow diet (Harlan; Cat# 2018). 3–4 month old wild-type and RTP801 (REDD1) knockout C57Bl/6x129SvEv mice (generated by Lexicon Inc.; Woodland, TX for Quark Pharmaceuticals Inc.; Fremont, CA) [20].

2.2. Intraperitoneal glucose tolerance (ipGTT) and insulin tolerance (ipITT) tests

Following a 12 h fast, blood glucose concentrations were determined through the tail vein. A small nick was made at the distal quarter of the tail with a sterile scalpel blade, and then a drop of blood was placed onto the test strip and measured by a handheld glucometer (OneTouch Ultra, LifeScan Inc.). At this time, blood loss was stopped by application of a styptic pencil to the nick area. Then 2 g/kg BW sterile glucose (Sigma) was administered via intraperitoneal (ip) injection with a sterile 0.3 mL syringe/26 gauge needle. The mouse was then returned to its cage until the next collection timepoint and every timepoint thereafter. Blood glucose was assessed by the same method described above at 15, 30, 60, 90, and 120 min.

Following a 6 h fast (to limit possible terminal reductions in blood glucose that may occur with a 12 h fast), blood glucose concentration was determined through the tail vein. Again, a small nick at the distal quarter of the tail was made on the tail vein with a sterile scalpel blade, then a drop of blood was placed onto the test strip and measured by a handheld glucometer (OneTouch Ultra, LifeScan Inc.). At this time, blood loss was stopped by application of a styptic pencil to the nick area. Next, 0.5 IU/kg BW insulin (Humulin, Eli Lilly) was administered by intraperitoneal injection with a sterile 0.3 mL syringe/26 gauge needle, and blood glucose was determined at 7.5, 15, 30, 45, and 90 min through the tail vein. The mouse was then returned to its cage until the next collection timepoint and every timepoint thereafter. Changes in glucose were plotted over time for both the ipGTT and ipITT, then the area under the curve (AUC) was also calculated [21].

2.3. Insulin injection

Following a 12 h fast, the animals were placed under 3.5% isoflurane anesthesia for the duration of the procedure. Then the right plantar flexor complex (containing the medial and lateral gastrocnemius, soleus, and plantaris muscles) was removed and immediately placed it in liquid nitrogen for subsequent analysis. Insulin (Humulin, Eli Lilly) was then injected into the intraperitoneal space at a concentration of 0.5 IU/kg BW. After 10 min, the remaining (left) plantar flexor complex was removed and placed immediately into liquid nitrogen for subsequent analysis.

2.4. Tissue homogenization

The plantar flexor complex muscle samples collected during the insulin injection protocol were homogenized in 10 volumes of CHAPS-containing buffer [40 mM HEPES (pH 7.5), 120 mM NaCl, 1 mM EDTA, 10 mM pyrophosphate, 10 mM-glycerophosphate, 40 mM NaF, 1.5 mM sodium vanadate, 0.3% CHAPS, 0.1 mM PMSF, 1 mM benzamidine, 1 mM DTT, and protease inhibitors (#04693116001, Roche, Indianapolis, IN)]. An initial aliquot of the homogenate, serving as a total muscle lysate, was collected for Western analysis. The homogenate was further clarified by a 1000*rcf* centrifugation for 5 min (at 4 °C), and the supernatant was retained (i.e. cytoplasmic enriched fraction). A small aliquot of each sample was taken for the determination of protein concentration for each sample. An equal volume of 2X sodium dodecyl sulfate loading buffer was added to each fraction, boiled for 5 min, then Western analysis was performed.

2.5. Western blotting

First, equal quantities of protein (Coomassie; Thermo) were resolved by sodium dodecyl sulfate–polyacrylamide gel electrophoresis (SDS–PAGE), and then transferred onto a PVDF membrane. After blocking in 5% non-fat milk in tris-buffered saline (TBS) plus 0.1% Tween-20 (TBS-T) for 1 h, membranes were incubated with anti-phospho primary antibodies (Cell Signaling) for Akt S473, Akt T308, IRS-1 Y1222, ERK 1/2 T202/Y204, S6K1 T389, or 4E-BP1 T37/46 and total antibodies for REDD1 (Proteintech), S6K1 (Cell Signaling), and GAPDH (Cell Signaling) in TBS-T overnight at 4 °C. Membranes were then washed and incubated with the respective secondary antibody for 1 h in a 5% non-fat milk/TBS-T solution at room temperature. The membranes were washed in TBS-T, then visualized via ECL and then quantified by measuring the luminescent signal using a Bio-Rad ChemiDoc MP Imager. The blots were analyzed using Bio-Rad Image Lab software and the data was expressed as a percentage of the respective control group for each individual blot.

2.6. Statistical analysis

Statistics were performed using IBM SPSS v22.0.0 software. The results are expressed as the mean ± standard error. Comparisons were made for each variable using independent or paired (where appropriate) two-tailed *t*-test or a one-way analysis of variance, Tukey HSD *post hoc* test, to establish significant differences between groups (only after the F statistic indicated an overall significance). The significance levels was set *a priori* at $p < 0.05$.

3. Results

3.1. Glucose and insulin tolerance

Though not significantly different from one another, the REDD1 KO mice had higher blood glucose concentrations after a 12 h fast (Fig. 1A), which is consistent with our previously reported findings [11]. However, 15 and 30 min after the glucose injection, blood glucose concentrations were significantly higher (Fig. 1A; $p < 0.05$) in the REDD1 KO mice when compared to the WT mice at those same timepoints. Thereafter, both the REDD1 WT and KO mice displayed similar blood glucose concentrations for the remainder of the test. Consistent with this, the area under the curve (AUC) was correspondingly higher (Fig. 1A Inset; $p < 0.05$) for the REDD1 KO versus the WT mice.

For the insulin tolerance test, the mice were fasted for only 6 h to limit detrimentally low glucose concentrations following insulin

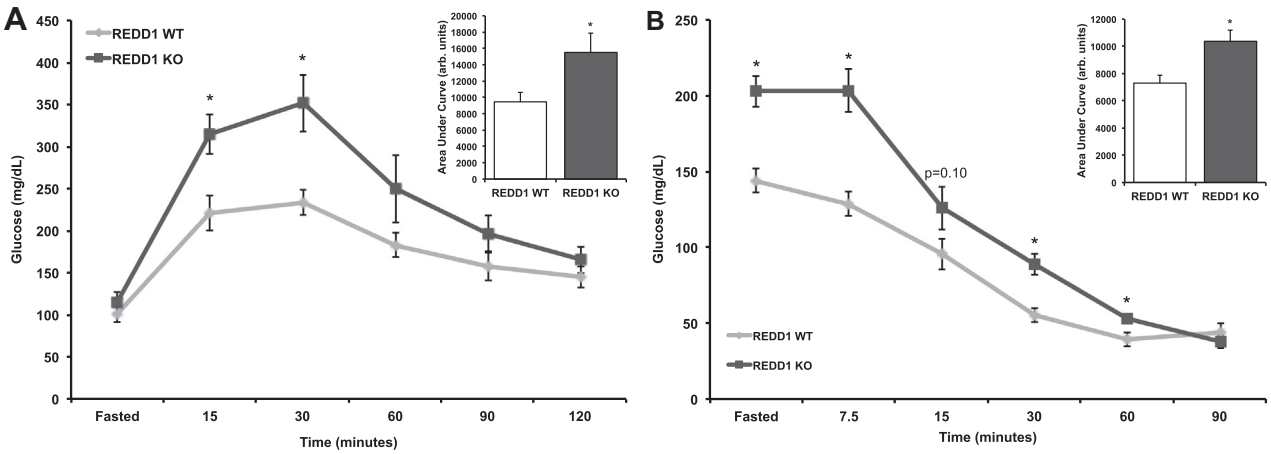

Fig. 1. Loss of REDD1 promotes glucose and insulin intolerance. In the fasted state, REDD1 wildtype (WT) and knockout (KO) mice were injected intraperitoneally (IP) with 2 g/kg BW glucose or 0.5 IU/kg BW insulin to determine whole body (A) glucose tolerance or (B) insulin tolerance, respectively. Upon determination of fasted blood glucose via the tail vein, glucose or insulin was injected, then glucose was monitored for the designated timepoints via the tail vein. See inset figure for the area under the curve (AUC) calculation data. Data are presented as mean ± standard error of the mean. $^{*}p < 0.05$ versus WT for the respective timepoint.

injection. Fasted blood glucose concentrations were now significantly higher (Fig. 1B; $p < 0.05$) in the REDD1 KO versus the WT mice. Insulin injection resulted in reductions of glucose for both groups though the REDD1 KO mice were higher (Fig. 1B; $p < 0.05$) at 7.5, 30, and 60 min when compared to the WT mice. Correspondingly, the AUC was significantly higher (Fig. 1B Inset; $p < 0.05$) in the REDD1 KO versus the WT mice.

3.2. Insulin stimulation

Consistent with our previous observations [10,11], skeletal muscle mTORC1 signaling was dysregulated under a fasted state. Phosphorylation of T37/46 on 4E-BP1 was higher (Fig. 2A; $p < 0.05$) in the plantar flexor complex muscle from fasted, non-stimulated (control) REDD1 KO mice when compared to Con WT mouse muscle. However, insulin stimulation had little effect on 4E-BP1 and S6K1 phosphorylation in the KO mice versus the WT mice (Fig. 2A and B). This corresponded to a control-to-insulin stimulated percent change of 36.7 ± 8.9% versus 4.8 ± 7.9% for 4E-BP1 phosphorylation ($p < 0.05$) and a 163.4.7 ± 48.0% versus 100.7 ± 10.6% for S6K1 T389 phosphorylation in the WT versus KO mice ($p < 0.05$), respectively. Confirmation of the skeletal muscle expression of REDD1 in the REDD1 WT and KO are presented in Fig. 2C.

Next, we examined skeletal muscle insulin signaling intermediate activation before and after insulin stimulation. Phosphorylation of the Y1222 residue on insulin receptor substrate-1 (IRS-1) was robustly increased (Fig. 3A; $p < 0.05$) by insulin stimulation in the REDD1 WT versus the REDD1 KO mice, that resulted in a control-to-insulin stimulated percent change of 830.3 ± 133.9% versus 233.0 ± 95.8% for IRS-1 phosphorylation in the WT versus KO mice ($p < 0.05$), respectively. Phosphorylation of Akt on the S473 site was significantly higher (Fig. 3B; $p < 0.05$) in the insulin stimulated versus the control in both the REDD1 WT and KO mice, though significantly lower ($p < 0.05$) insulin stimulated Akt S473 phosphorylation in the REDD1 KO mouse muscle compared to REDD1 WT. Similarly, phosphorylation of Akt on the T308 site was significantly higher in both the REDD1 WT and KO mice following insulin treatment (Fig. 3C; $p < 0.05$) versus the control leg of the REDD1 WT mice. The insulin stimulated muscle from the REDD1 KO mice trended lower ($p = 0.09$; Fig. 3C) when compared to the WT insulin stimulated muscle. Overall lower control and insulin stimulated responses in the REDD1 KO mice resulted in a similar control-to-insulin stimulated percent changes of 723.3 ± 125.9% versus 846.4 ± 281.1% for the total homogenate Akt S473 and 1190.1 ± 155.3% versus 1417.4 ± 501.7% for total homogenate Akt T308 phosphorylation in the WT versus KO mice, respectively. When the cytosolic fraction was examined for Akt S473 and T308 phosphorylation, results comparable to those established in the total fraction were observed (data not shown). Lastly, the insulin stimulated phosphorylation of ERK 1/2 was lower (Fig. 4; $p < 0.05$) in the muscle from REDD1 KO versus the WT mice, yielding a control-to-insulin stimulated percent change of 5415.4 ± 1813.6% versus 156.3 ± 79.6% for ERK 1/2 phosphorylation in the WT versus KO mice ($p < 0.05$), respectively.

4. Discussion

Our recent findings [11] show that despite hyperactive mTORC1 signaling in skeletal muscle from fasted REDD1 knockout mice, fed knockout mouse muscle did not exhibit a robust increase in mTORC1 signaling activation like their fed wildtype counterparts. Thus, our data suggested that a lack of REDD1 alters the ability to appropriately respond to nutrient cues. Therefore, our goal with this study was to determine the role of REDD1 on whole body glucose and insulin tolerance and skeletal muscle insulin action. The current findings provide strong support that REDD1 regulates whole body and skeletal muscle insulin action.

Insulin is central to the stimulation of glucose uptake from circulating blood into skeletal muscle, among other tissues, primarily through signaling regulated by the insulin receptor. Upon insulin binding to its receptor, a series of signaling events result in the translocation of the glucose transporter, GLUT4, to the cell membrane. Central to this process is the activation of the IRS-1 and subsequent activation of the PI3K and ERK1/2 pathways promoting glucose uptake, as well as cell proliferation, growth, and survival [3]. Here we show that a loss of total body REDD1 results in impaired glucose and insulin tolerance, evident by the higher blood glucose concentrations observed in the REDD1 KO mice after glucose and insulin injections, respectively. An interesting point to make is that the fasted blood glucose levels were higher in the KO mice prior to the insulin tolerance test, but not the glucose tolerance test. This may be due to the time of fast (6 versus 12 h). In support of this, in our previous report [11], the REDD1 KO mice had non-significantly higher fasted blood glucose concentrations at both 12 and 18 h, which further support metabolic dysfunction

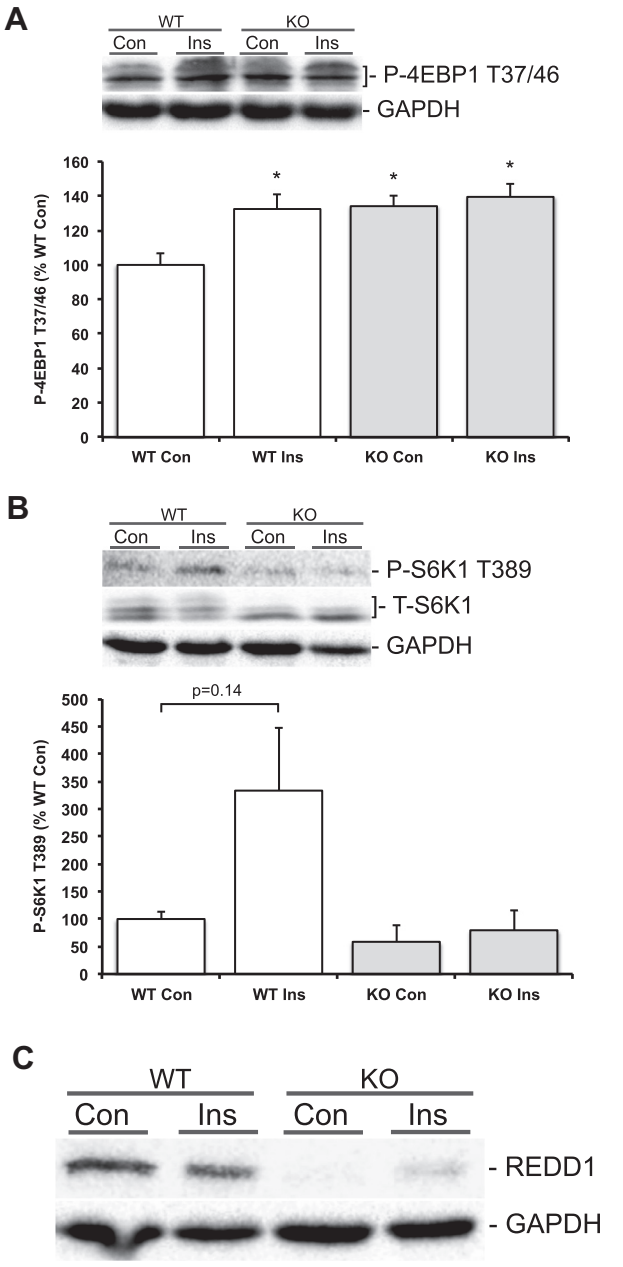

Fig. 2. Loss of REDD1 promotes dysregulated mTORC1 signaling. Initially, a plantar flexor complex muscle group from fasted REDD1 wildtype (WT) and knockout (KO) mouse was removed and frozen in liquid nitrogen while under anesthesia. Remaining under anesthesia, the mice were IP injected with 0.5 IU/kg BW insulin, and after 10 min the remaining plantar flexor complex muscle group was removed and frozen in liquid nitrogen. The cytosolic fraction from the muscle homogenate was analyzed by Western analysis for (A) phospho-4E-BP1 T37/46, (B) phospho-S6K1 T389 and total S6K1, (C) REDD1, and normalized to GADPH. $^{*}p < 0.05$ versus fasted WT.

in the REDD1 KO model. Based upon the current findings reported herein, these data strongly support the contention that skeletal muscle glucose uptake would be lower in the REDD1 KO mice, though this cannot be concluded. A determination of glucose uptake into skeletal muscle would directly support this statement and the glucose and insulin intolerance observed in the REDD1 KO mice, though was not measured in the current study. The role of REDD1 in glucose metabolism represents an important issue that remains unexplored, though is outside the scope of the current study.

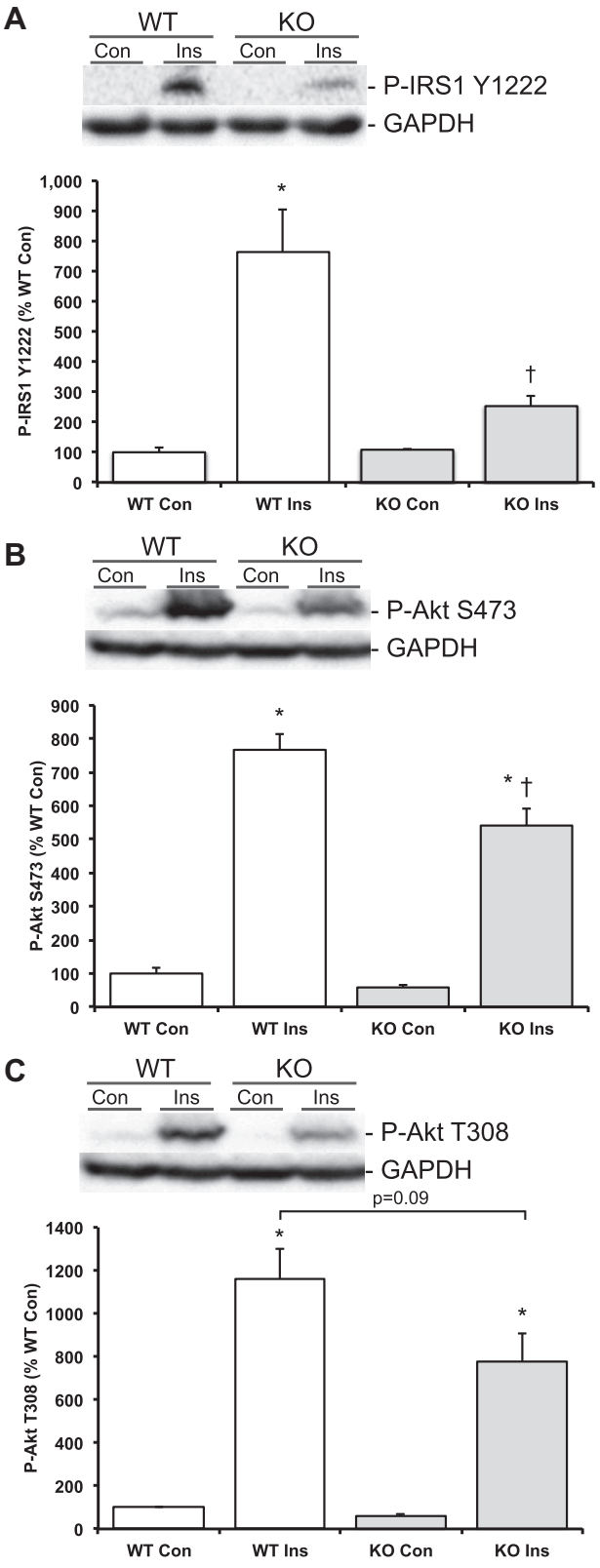

Fig. 3. Loss of REDD1 promotes dysregulated insulin stimulated IRS-1 signaling. Initially, a plantar flexor complex muscle group from fasted REDD1 wildtype (WT) and knockout (KO) mouse was removed and frozen in liquid nitrogen while under anesthesia. Remaining under anesthesia, the mice were IP injected with 0.5 IU/kg BW insulin, and after 10 min the remaining plantar flexor complex muscle group was removed and frozen in liquid nitrogen. The total muscle homogenates was analyzed by Western analysis for (A) phospho-IRS-1 Y1222, (B) phospho-Akt S473, (C) phospho-Akt T308, and normalized to GADPH. $^{*}p < 0.05$ versus WT Con and $^{\dagger}p < 0.05$ versus WT Ins.

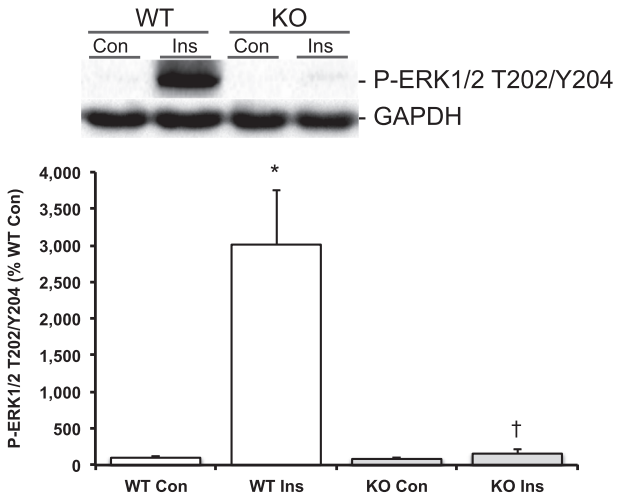

Fig. 4. Loss of REDD1 promotes dysregulated insulin stimulated ERK 1/2 phosphorylation. Initially, a plantar flexor complex muscle group from fasted REDD1 wildtype (WT) and knockout (KO) mouse was removed and frozen in liquid nitrogen while under anesthesia. Remaining under anesthesia, the mice were IP injected with 0.5 IU/kg BW insulin, and after 10 min the remaining plantar flexor complex muscle group was removed and frozen in liquid nitrogen. The cytosolic fraction from the muscle homogenate was analyzed by Western analysis for phospho-ERK 1/2 T202/Y204 and normalized to GADPH. $^{*}p < 0.05$ versus WT Con and $^{\dagger}p < 0.05$ versus WT Ins.

Consistent with the glucose and insulin intolerance and a low insulin-stimulated response of mTORC1 substrates, 4E-BP1 and S6K1 (versus the WT), insulin stimulation of IRS-1 on tyrosine residues was severely blunted in the REDD1 KO mouse muscle. When mTORC1 signaling is hyperactive it serves to negatively feedback and downregulate IRS-1 and its substrates, possibly contributing to reduced insulin action [4]. More germane to cell growth, insulin stimulates the PI3K and Ras pathway and promotes activation of Akt and ERK1/2, respectively, phosphorylating and inactivating TSC2. Inactivation of the TSC complex will promote Rheb GTPase activity and subsequent activation of mTOR.

For cell, animal, and human models examining insulin action or skeletal muscle growth signaling pathway activation, Akt phosphorylation has been a common target kinase. The IRS-1/PI3K/Akt pathway activation by insulin regulates glucose metabolism, as well as mTORC1 signaling. Though not significant, Akt S473 and T308 phosphorylation was lower in the fasted REDD1 KO mouse muscle when compared to the WT, which is similar to ours [11] and others [22] previous findings. The lack of significance in this case may be due to the rather large increases observed with the insulin treatment, limiting our ability to detect smaller changes. Despite increases in Akt S473 and T308 phosphorylation following stimulation, the REDD1 KO mice displayed less of an increase when compared to the WT mice. Upon activation, Akt can translocate to the plasma membrane and the nucleus, as well as remain in the cytosol. Given this, we examined the total muscle homogenate and the cytosolic fraction from muscle (data not shown), yielding similar results. A recent report from Dennis et al. [19] show preferential insulin stimulation of the T308 versus the S473 site on Akt. The authors report [19] that a loss of REDD1 limits insulin's ability to stimulate Akt on the S473 site, whereas phosphorylation of the T308 site was amplified in the REDD1−/− MEFs in response to insulin treatment. Current models suggest that phosphorylation of T308 on Akt is PDK1-dependent, whereas the S473 site is mTORC2-dependent. Work from Regazzetti et al. [23] show a reduction in Akt T308 phosphorylation during REDD1 knockdown in adipocytes. Possible differences between the current and abovementioned findings that might influence Akt site-specific phosphorylation could be the cell type (MEF versus muscle versus adipocyte), whole body versus individual cell experiments, the length of insulin activation (10 min versus 30 min), model of REDD1 loss (genetic loss versus siRNA knockdown), or fraction examined (total versus cytosolic). Independent of fraction examined, the current data suggest that a whole body loss of REDD1 limits muscle Akt phosphorylation in response to insulin stimulation.

Insulin's ability to promote activation of the ERK1/2 pathway through Ras has been well established, though less has been reported as it relates to REDD1. Insulin can promote REDD1 expression [23,24], possibly to limit mTORC1 signaling. Recent findings [23] support this contention by showing that insulin regulates REDD1 degradation and subsequent control of mTORC1 through a MEK1/2-sensitive mechanism. The authors also report that low REDD1 expression reduces insulin's ability to phosphorylate IRS-1, Akt, and ERK1/2, which corroborate our current findings. Interestingly, ERK1/2 can phosphorylate TSC2 on S644, inactivating the TSC complex, and the autoinhibitory domain (T421/S424) on S6K1, promoting mTORC1 signaling activation [4]. Also, reports suggest that 4E-BP1 may be regulated by ERK1/2, controlling mRNA translation. Consistent with 4E-BP1, a lack of REDD1 resulted in reduced insulin-stimulated S6K1 T389 phosphorylation. However, we did not observe a higher S6K1 phosphorylation under fasted conditions as we have previously reported [10,11], which may be due to the length of the fast (12 versus 18 h). As mentioned above, REDD1 regulates Akt T308 phosphorylation through a PP2A mechanism [19]. The ERK pathway can also be regulated by PP2A, as well as other phosphatases such as PTP and MKP [25], suggesting overlapping means of regulation by REDD1 upon insulin stimulation.

Our results herein extends our previous findings [11] that a lack of REDD1 limits mTORC1 signaling response to a growth stimulus. The results provide a deeper understanding of REDD1 as it relates to insulin-stimulated mTORC1 signaling, encompassing metabolism and insulin action. A lack of REDD1 contributes to glucose and insulin intolerance that is associated with dysregulated insulin stimulation of both mTORC1 and ERK1/2 pathways.

Support

This research was supported by University at Buffalo, SUNY (DLW).

Conflict of interests

The authors have no conflict of interests to report.

Acknowledgments

The authors would like to thank Drs. Elena Feinstein and Rubin Tuder for providing the REDD1 knockout mouse breeding pair. Also, the authors thank Dr. John Wilson for laboratory equipment use. A thank you to the Confocal Microscope and Flow Cytometry Facility for equipment use. Due to space limitations, we may have omitted certain references.

References

[1] D.E. Alley, V.W. Chang, The changing relationship of obesity and disability, 1988–2004, JAMA 298 (2007) 2020–2027.
[2] P. Srikanthan, A.S. Karlamangla, Relative muscle mass is inversely associated with insulin resistance and prediabetes. Findings from the third National Health and Nutrition Examination Survey, J. Clin. Endocrinol. Metab. 96 (2011) 2898–2903.
[3] J. Boucher, A. Kleinridders, C.R. Kahn, Insulin receptor signaling in normal and insulin-resistant states, Cold Spring Harb. Perspect. Biol. 6 (2014).
[4] M. Laplante, D.M. Sabatini, mTOR signaling in growth control and disease, Cell 149 (2012) 274–293.

[5] S.R. Kimball, L.S. Jefferson, P. Fadden, T.A.J. Haystead, J.C. Lawrence, Insulin and diabetes cause reciprocal changes in the association of eIF4E AND PHAS-I rat skeletal muscle, Am. J. Physiol. 270 (1996) C705–C709.
[6] D.H. Kim, D.D. Sarbassov, S.M. Ali, J.E. King, R.R. Latek, H. Erdjument-Bromage, P. Tempst, D.M. Sabatini, mTOR interacts with raptor to form a nutrient-sensitive complex that signals to the cell growth machinery, Cell 110 (2002) 163–175.
[7] D.D. Sarbassov, S.M. Ali, S. Sengupta, J.H. Sheen, P.P. Hsu, A.F. Bagley, A.L. Markhard, D.M. Sabatini, Prolonged rapamycin treatment inhibits mTORC2 assembly and Akt/PKB, Mol. Cell 22 (2006) 159–168.
[8] P.E. Burnett, R.K. Barrow, N.A. Cohen, S.H. Snyder, D.M. Sabatini, RAFT1 phosphorylation of the translational regulators p70 S6 kinase and 4E-BP1, Proc. Natl. Acad. Sci. U.S.A. 95 (1998) 1432–1437.
[9] S.H. Um, F. Frigerio, M. Watanabe, F. Picard, M. Joaquin, M. Sticker, S. Fumagalli, P.R. Allegrini, S.C. Kozma, J. Auwerx, G. Thomas, Absence of S6K1 protects against age- and diet-induced obesity while enhancing insulin sensitivity, Nature 431 (2004) 200–205.
[10] J.C. Drake, S.E. Alway, J.M. Hollander, D.L. Williamson, AICAR treatment for 14 days normalizes obesity-induced dysregulation of TORC1 signaling and translational capacity in fasted skeletal muscle, Am. J. Physiol. Regul. Integr. Comp. Physiol. 299 (2010) R1546–R1554.
[11] D.L. Williamson, Z. Li, R.M. Tuder, E. Feinstein, S.R. Kimball, C.M. Dungan, Altered nutrient response of mTORC1 as a result of changes in REDD1 expression: effect of obesity vs. REDD1 deficiency, J. Appl. Physiol. 1985 (117) (2014) 246–256.
[12] F. Tremblay, A. Gagnon, A. Veilleux, A. Sorisky, A. Marette, Activation of the mammalian target of rapamycin pathway acutely inhibits insulin signaling to Akt and glucose transport in 3T3-L1 and human adipocytes, Endocrinology 146 (2005) 1328–1337.
[13] L.W. Ellisen, K.D. Ramsayer, C.M. Johannessen, A. Yang, H. Beppu, K. Minda, J.D. Oliner, F. McKeon, D.A. Haber, REDD1, a developmentally regulated transcriptional target of p63 and p53, links p63 to regulation of reactive oxygen species, Mol. Cell 10 (2002) 995–1005.
[14] J. Brugarolas, K. Lei, R.L. Hurley, B.D. Manning, J.H. Reiling, E. Hafen, L.A. Witters, L.W. Ellisen, W.G. Kaelin Jr., Regulation of mTOR function in response to hypoxia by REDD1 and the TSC1/TSC2 tumor suppressor complex, Genes Dev. 18 (2004) 2893–2904.
[15] H. Wang, N. Kubica, L.W. Ellisen, L.S. Jefferson, S.R. Kimball, Dexamethasone represses signaling through the mammalian target of rapamycin in muscle cells by enhancing expression of REDD1, J. Biol. Chem. 281 (2006) 39128–39134.
[16] L. Lin, Y. Qian, X. Shi, Y. Chen, Induction of a cell stress response gene RTP801 by DNA damaging agent methyl methanesulfonate through CCAAT/enhancer binding protein, Biochemistry 44 (2005) 3909–3914.
[17] Z. Wang, M.H. Malone, M.J. Thomenius, F. Zhong, F. Xu, C.W. Distelhorst, Dexamethasone-induced gene 2 (dig2) is a novel pro-survival stress gene induced rapidly by diverse apoptotic signals, J. Biol. Chem. 278 (2003) 27053–27058.
[18] N.K. McGhee, L.S. Jefferson, S.R. Kimball, Elevated corticosterone associated with food deprivation upregulates expression in rat skeletal muscle of the mTORC1 repressor, REDD1, J. Nutr. 139 (2009) 828–834.
[19] M.D. Dennis, C.S. Coleman, A. Berg, L.S. Jefferson, S.R. Kimball, REDD1 enhances protein phosphatase 2A-mediated dephosphorylation of Akt to repress mTORC1 signaling, Sci. Signal. 7 (2014) ra68.
[20] A. Brafman, I. Mett, M. Shafir, H. Gottlieb, G. Damari, S. Gozlan-Kelner, V. Vishnevskia-Dai, R. Skaliter, P. Einat, A. Faerman, E. Feinstein, T. Shoshani, Inhibition of oxygen-induced retinopathy in RTP801-deficient mice, Invest. Ophthalmol. Vis. Sci. 45 (2004) 3796–3805.
[21] M.S. Beaudoin, L.A. Snook, A.M. Arkell, J.A. Simpson, G.P. Holloway, D.C. Wright, Resveratrol supplementation improves white adipose tissue function in a depot-specific manner in Zucker diabetic fatty rats, Am. J. Physiol. Regul. Integr. Comp. Physiol. 305 (2013) R542–R551.
[22] M.D. Dennis, N.K. McGhee, L.S. Jefferson, S.R. Kimball, Regulated in DNA damage and development 1 (REDD1) promotes cell survival during serum deprivation by sustaining repression of signaling through the mechanistic target of rapamycin in complex 1 (mTORC1), Cell. Signal. 25 (2013) 2709–2716.
[23] C. Regazzetti, F. Bost, Y. Le Marchand-Brustel, J.F. Tanti, S. Giorgetti-Peraldi, Insulin induces REDD1 expression through hypoxia-inducible factor 1 activation in adipocytes, J. Biol. Chem. 285 (2012) 5157–5164.
[24] R.A. Frost, D. Huber, A. Pruznak, C.H. Lang, Regulation of REDD1 by insulin-like growth factor-I in skeletal muscle and myotubes, J. Cell. Biochem. 108 (2009) 1192–1202.
[25] M.R. Junttila, S.P. Li, J. Westermarck, Phosphatase-mediated crosstalk between MAPK signaling pathways in the regulation of cell survival, FASEB J. 22 (2008) 954–965.